Alternating layer addition approach to CdSe/CdS core/shell quantum dots with near-unity quantum yield and high on-time fractions

Published in final edited form as:

Chem Sci. 2012 June 1; 3(6): 2028–2034. doi:10.1039/C2SC00561A.

Alternating layer addition approach to CdSe/CdS core/shell quantum dots with near-unity quantum yield and high on-time fractions

Andrew B. Greytak[a,b], **Peter M. Allen**[a], **Wenhao Liu**[a], **Jing Zhao**[a], **Elizabeth R. Young**[a], **Zoran Popović**[a], **Brian Walker**[a], **Daniel G. Nocera**[a], and **Moungi G. Bawendi**[a]

Andrew B. Greytak: greytak@chem.sc.edu; Daniel G. Nocera: nocera@mit.edu; Moungi G. Bawendi: mgb@mit.edu

[a]Department of Chemistry, Massachusetts Institute of Technology, 77 Massachusetts Avenue, Cambridge, Massachusetts, USA

Abstract

We report single-particle photoluminescence (PL) intermittency (blinking) with high on-time fractions in colloidal CdSe quantum dots (QD) with conformal CdS shells of 1.4 nm thickness, equivalent to approximately 4 CdS monolayers. All QDs observed displayed on-time fractions > 60% with the majority > 80%. The high-on-time-fraction blinking is accompanied by fluorescence quantum yields (QY) close to unity (up to 98% in an absolute QY measurement) when dispersed in organic solvents and a monoexponential ensemble photoluminescence (PL) decay lifetime. The CdS shell is formed in high synthetic yield using a modified selective ion layer adsorption and reaction (SILAR) technique that employs a silylated sulfur precursor. The CdS shell provides sufficient chemical and electronic passivation of the QD excited state to permit water solubilization with greater than 60% QY via ligand exchange with an imidazole-bearing hydrophilic polymer.

Introduction

Colloidal quantum dots (QDs) are a powerful class of semiconductor nanostructures exhibiting high photoluminescence quantum yields, large molar extinction coefficients, high photostability compared to typical organic molecular fluorophores, and size-tunable emission wavelengths that can extend across the visible to mid-IR spectral range.[1–3] These properties make QDs attractive candidates as biological fluorescent probes,[4–8] especially since their exceptional brightness and stability enables single molecule tracking over extended periods of time.[9]

Correspondence to: Andrew B. Greytak, greytak@chem.sc.edu; Daniel G. Nocera, nocera@mit.edu; Moungi G. Bawendi, mgb@mit.edu.

[b]Present address: Department of Chemistry and Biochemistry, University of South Carolina, 631 Sumter Street, Columbia, South Carolina, USA.

†Electronic Supplementary Information (ESI) available: Experimental methods, size calibration data, transmission electron microscopy, elemental analysis, and additional absorption spectroscopy. See DOI: 10.1039/b000000x/

‡Footnotes should appear here. These might include comments relevant to but not central to the matter under discussion, limited experimental and spectral data, and crystallographic data.

Core-shell heterostructures have been widely explored[10–14] as a means to adjust the photophysical properties of QDs, and can be used to increase their brightness as fluorophores in two ways: (1) maximizing the photoluminescence quantum yield (QY) through electronic and chemical isolation of the core from surface-associated recombination centers;[11,13,15] and (2) increasing the excitation rate (absorption cross-section) by building a high density of electronic states at energies above the shell bandgap.[14–16] These two roles for the shell present a potential trade-off in terms of shell material. A wide bandgap shell imposes large electronic barriers for carrier access to the surface but will be less able to contribute to absorption, while a narrower gap shell could participate in light harvesting but may make it harder to achieve high QY. Shell thickness can also be increased, but this comes at the expense of increased total size, which may be undesirable, particularly in biological applications.

For the case of CdSe, one of the best studied nanocrystal QD core materials, CdS and ZnS are isostructural materials that have been applied to form shells,[11,12,14–18] both as pure materials and in heterostructures with alloyed and/or graded compositions of $Cd_xZn_{1-x}S$.[17] The use of Cd-rich or pure CdS shells imposes challenges in maintaining high QY,[17,18] and in terms of the strong redshift of the QD excited states encountered upon overcoating with a weakly-confining shell.[19] The redshift imposes a strong requirement of structural homogeneity in shell growth if inhomogeneous broadening of the photoluminescence (PL) emission spectrum is to be avoided. In order to help suppress nucleation and anisotropic elaboration[16,20] of the nanocrystals, selective ionic layer adhesion and reaction (SILAR) growth techniques have been applied.[15,17,18,21,19]

Fluorescence intermittency (blinking) of individual QDs affects their performance as single-molecule fluorescent tracers and in other applications. Much effort has been devoted to understanding the mechanisms of blinking in colloidal QDs[22,23] and to identifying structures that can suppress it. Recently, several groups have reported suppression of blinking in CdSe/CdS core/shell QDs with thick (4–6 nm) shells.[15,21,24] Despite single-particle fluorescence data indicating high on-time fractions and a near-unity QY with mono-exponential decay in the on state,[24] the reported ensemble QYs are 50–70%,[15,24] indicating that the high-excitation-fluence single particle statistics are not necessarily representative of ensemble behavior at lower fluence. An important question is whether such high on-time fractions can be achieved for QDs with thinner CdS shells (and thus smaller total diameter), and if so, whether a correspondingly high ensemble QY can be maintained in solution samples.

In the work described below, we use a SILAR approach to grow CdSe/CdS core/shell QDs that display near-unity quantum yields in organic solution. Among two samples with differing core radii and emission wavelengths, individual QDs universally displayed high on-time fractions in single-particle blinking experiments. We also report ligand-exchange experiments that show significant retention of ensemble QY (> 60%) when the QDs are brought into aqueous solution. We observe nearly quantitative conversion of shell growth reagents, which aids in programming of desired photoluminescence characteristics in the resulting particles and limits waste. This result contributes to a growing body of work on CdS-coated CdSe QDs[15,21,25,26,19] that promises to provide a set of very bright and compact

inorganic fluorophores and to open new applications that take advantage of the relaxed confinement conditions[16,27] found with narrower-bandgap shell materials.

Experimental Design

Conformal shells on nanocrystals are generally produced by introducing shell precursors in a manner such that material adds to the surface of existing nanocrystals but nucleation of new particles is rejected.[11] In the SILAR approach to shell growth, metal and chalcogenide precursors are added separately, in an alternating fashion.[18] The goals of such an approach are to: (1) saturate available surface binding sites in each half-cycle in order to enforce isotropic shell growth; and (2) avoid the simultaneous presence of both precursors in solution so as to minimize the rate of homogenous nucleation of new nanoparticles of the shell material. These goals are potentially at cross purposes: the use of a large excess of precursor in each half-cycle (as is common in SILAR on planar substrates[28,29]) would be desirable to drive saturation of surface binding sites, but for the case of nanocrystals in homogeneous solution, any excess reagent cannot be easily removed and may linger until the next half-step, potentially leading to nucleation of particles of the shell material and/or uncontrolled surface growth on the existing cores. As a result, reagent doses for SILAR on nanocrystals are generally calculated with the goal of providing exactly one monolayer (ML) of coverage,[18] and sometimes with a slight excess designed to make up for incomplete reaction of the shell precursors.[19]

The value of 0.337 nm, or half of the wurtzite *c*-axis unit cell dimension for CdS, is considered here to be the marginal increase in radius associated with 1 monolayer (ML) of surface coverage. This value is necessarily approximate, but is in wide use in the SILAR literature.[15,18] Moreover, X-ray photoelectron spectroscopy measurements of CdSe/ZnS nanocrystals have shown that, taking one half of the wurtzite *c*-axis unit cell for ZnS as a yardstick, 1.2 ML was sufficient to suppress Se oxidation on exposure to ambient air, while 0.65 ML was not.[13]

The most common method for producing CdSe/CdS core/shell QDs via SILAR, as developed by Peng,[18] starts with CdSe cores synthesized from the reaction of Cd carboxylates and trialkylphosphine selenides. The shell precursors are typically Cd oleate and elemental S, each dissolved in octadecene, and these are introduced in an alternating fashion and allowed to react at 240 °C.

We employed a modified SILAR approach for shell growth, in which alternating layer addition was performed at constant temperature using hexamethyldisilathiane (TMS_2S) as the sulfur precursor, and with sub-monolayer reagent doses in each half-cycle. These choices were made with the aim of maximizing the synthetic yield for shell growth, and suppressing any nucleation of particles composed of the shell material. In particular, the use of TMS_2S as the S precursor could play a role in silylating carboxylate- and phosphonate-based ligands[30] and thereby deprotecting the nanocrystal surface in a manner analogous to that recently noted for the use of trimethylsilyl groups in driving ligand exchange reactions at nanocrystal surfaces.[31] While TMS_2S is well known as a precursor for sulphide shells on QDs under simultaneous addition alongside alkylated metal sources, its use in SILAR is

atypical.[11–13] We chose to apply doses equivalent to approximately 0.8 ML incremental shell thickness (= 0.27 nm) in each SILAR cycle.

Complete synthetic details are available in the Supplementary Information (ESI). We synthesized CdSe nanocrystal cores using cadmium oxide and trioctylphosphine selenide precursors in the presence of tetradecylphosphonic acid (TDPA) in a solvent of trioctylphosphine (TOP) and trioctylphosphine oxide (TOPO).

Overcoating by SILAR was accomplished at a constant temperature of 180°C in a solvent of oleylamine and 1-octadecene (ODE). The cadmium precursor was Cd oleate in a solvent of 50:50 ODE and TOP with two equivalents of 1-decylamine (vs. Cd) added. The sulfur precursor, TMS_2S, was dissolved in TOP. CdSe cores were isolated by repeated flocculation from hexane with acetone. The core radius was estimated using a calibration curve[32] (see also ESI, Fig. S1) for radius as a function of the position of the lowest-energy absorption peak. The quantity (number of moles) of cores in a given sample was determined by estimating the molar extinction coefficient based on this radius in the manner of Leatherdale et al.[33] The dose of Cd and S precursors required for each SILAR step was determined by dividing the incremental volume associated with each cycle of shell growth by the CdS unit cell volume (0.101 nm^3)[34] and scaling to the total number of cores. The Cd and S doses for each cycle are equal, while doses for successive cycles increase geometrically according to the increasing marginal volume associated with equal increments in radius.

Following shell growth, the solution was quantitatively recovered; under the condition that the number of particles does not change, this allows the molar extinction coefficient of the overcoated QDs to be determined from the measured absorption spectrum. The progress and yield of the overcoating reaction were monitored via UV-VIS absorption, PL, transmission electron microscopy (TEM), and wavelength dispersive spectroscopy (WDS) compositional analysis. Experimental details of these measurements, and of the time-resolved PL measurements and ligand exchange procedures, are found in the Supplementary Information.

Results and Discussion

Nanocrystal synthesis and shell growth

We have performed several variations of our synthetic procedure to produce CdSe/CdS core/shell nanocrystals with different core sizes and shell thicknesses, allowing tuning of the emission wavelength and other properties. Table 1 describes three representative samples that will be discussed here. Samples **1A** and **1B** are different thickness shells (5 and 4 cycles, respectively) made using two aliquots of the same CdSe core batch, while sample **2** features 5 cycles of CdS shell growth applied to longer-wavelength CdSe cores.

Figure 1(a) shows the change in the absorption spectrum associated with each full cycle of shell growth for sample **1A**, as measured by drawing small aliquots and diluting them in hexane. The CdSe cores used exhibited a lowest-energy exciton absorption feature at 487 nm, and showed a well-resolved band-edge PL peak at 503 nm, but low PL QY, when dispersed in hexanes.

We found a small redshift in absorption after each Cd injection, and a greater change after addition of S (see also ESI, Fig. S2). In both cases, the change was complete within 5 minutes following each injection; a total of 15 minutes between start times was allowed for each half-cycle. Addition of a total of 5 aliquots each of Cd and S yielded QDs with emission at 570 nm and a full width at half maximum (fwhm) of 25 nm. The redshifted absorption and PL spectra (Fig. 1(a,b)), the maintenance of a narrow PL lineshape, and the dramatic increase in absorption at blue wavelengths are consistent with the formation of a CdS shell and indicative of a high degree of structural homogeneity. By changing the CdSe core radius and the CdS shell thickness as exemplified in Table 1, we were able to tune the PL emission peak wavelength over nearly 50 nm among samples; the energy shifts that we observe with increasing CdS shell thickness, as shown in Fig. 1c, are comparable to those reported in the literature.[19]

TEM imaging revealed a relatively homogeneous set of roughly spherical particles (see ESI, Fig. S3). For sample **1A**, the volume-average radius was 2.8 nm. This slightly exceeds the predicted radius of 2.7 nm based on the estimated core radius of 1.3 nm and the targeted shell thickness of 1.4 nm. Elemental analysis of sample **1B** by WDS revealed Cd:Se and S:Se ratios consistent with a shell thickness of 1.0 nm, which is > 90% of the targeted shell thickness of 1.1 nm (see ESI, Table S1 and Fig. S4). These results support a high synthetic yield for incorporation of the shell precursors into the QDs. Importantly, nucleation of CdS particles was not observed. These observations are consistent with our expectations as described in the previous section, but a detailed study of the dependence of synthetic yield and morphology on reagent source and dose are beyond the scope of the present work.

To explore the effect of introducing an additional ZnS shell to form CdSe/CdS/ZnS core/shell/shell heterostructures, we isolated a portion of sample **1B** and treated it with alternating doses of diethylzinc (in ODE/TOP) and TMS_2S precursors, under conditions similar to those employed for CdS shell growth above. While the synthetic yield for ZnS shell formation was much lower than for CdS (as revealed by WDS elemental analysis data, see ESI), it was sufficient to cause significant changes in the photophysical properties as discussed below. Figure 2 shows the molar extinction spectrum of sample **1B** before and after application of the ZnS shell, revealing an increase in the absorption coefficient at short wavelengths with little shift in the band-edge exciton energy.

Ensemble QY and time-resolved ensemble PL

All samples showed striking increases in brightness under room light upon overcoating with CdS, as was expected. The absolute PL QY of sample **1B** was 98% as measured using an integrating sphere under 514 nm excitation; characteristic values among similarly prepared samples fall between 90% and 98%. This marks a significant increase compared to most previously-reported CdSe/CdS core/shell examples. Table S2 (see ESI) summarizes results from literature and from the present work. While QY approaching 100% has been reported for CdSe/CdS QDs under simultaneous addition, this was based on a relative, rather than absolute, QY measurement, and a maximum of 60–70% is characteristic among shells formed by alternating-layer growth, including in samples used in studies designed to probe quantum dot photophysics. The formation of samples displaying near-unity ensemble QY

can potentially simplify interpretation of time-resolved measurements and ultimately lead to a better understanding of the structural features that lead to excited-state quenching and the synthetic steps that can control the occurrence of such features.

Time-resolved PL spectroscopy was employed to characterize the excited state decay process in CdSe/CdS core/shell samples displaying high ensemble QY. Figure 3 displays the ensemble PL decay from sample **1B** diluted in hexanes at room temperature, excited at low power (exciton density $n < 0.1$) with pulsed 400 nm radiation from a Ti:sapphire laser and recorded using a streak camera. The decay trace is well-described with a single exponential lifetime τ of ~26 ns. Fluorescence intermittency (blinking) measurements have previously shown that in single QDs, intensity fluctuations are chiefly due to time-varying nonradiative rates and that at maximally bright timepoints, QDs can display near-unity QY and monoexponential PL decays dominated by the radiative recombination rate.[35,36,24] An ensemble QD sample displaying near-unity QY is therefore expected to show largely mono-exponential excited-state decay kinetics because the radiative decay rate, determined by band-edge electronic structure[37], should be homogeneous in a structurally homogeneous sample. The mono-exponential decay that we observe at low excitation power is thus consistent with expectations based on the high ensemble QY, but is also indicative of consistent radiative rates among the ensemble population.

When the QDs described here are excited at high fluence (average exciton density per particle $n \approx 2$), an intense decay component is observed with a spectrum similar to that at low fluence and a lifetime of < 100 ps (sample **1B**, Fig. 4); we interpret this as a rapid biexciton decay due to Auger recombination.[38,39]

Single-particle blinking

To characterize blinking in our high QY samples, we observed single QDs from samples **1A** and **2** at room temperature under continuous-wave excitation at 514 nm. An excitation power density of ~130 W-cm^{-2} was estimated to provide excitation rates of 2×10^5 s^{-1} and 3.4×10^5 s^{-1} for samples **1A** and **2** respectively Representative PL intensity traces (Fig. 5(a,c)) reveal well-resolved binary blinking between on- and off-state values, and high on-time fractions of 93% (Fig. 5(a)) and 90% (Fig. 5(c)). All QDs observed in each sample displayed on-time fractions > 60% with the majority > 80% (Fig. 5(b,d)).

Models for fluorescence intermittency in QDs have often proposed that the off state is characterized by the persistent presence of extra carrier(s) in one of the band-edge spherical-well states (resulting in an off-state QY that is limited by Auger recombination),[22] and/or by the opening of non-radiative decay pathway(s) via localized trap state(s).[23] In the first of these, trapping is only responsible for switching between on- and off-states, while in the second, trapping is responsible for quenching (at least at low fluence).

The large blinking modulation depth (> 90%) and binary switching that we observe suggest that a single charging or trap-opening event is sufficient to bring the QD into the off state, but given the short biexciton lifetime measured for our samples in the ensemble measurement, we cannot rule out either of the above quenching mechanisms.

The on-time fraction is not necessarily a robust metric by which to compare samples; switching rates are power-dependent and higher excitation rates can lead to diminished on-time fractions. Nonetheless, the >80% on-time fraction found here is significantly higher than those typically reported in studies of CdSe/ZnS and CdSe/CdS QDs at similar shell thickness and at similar excitation rates.[40,41]

Our results can be discussed in the context of reports of suppression of blinking in CdSe/CdS core/shell QDs with thick (4–6 nm) shells[15,21,24] that have emerged in recent years. Such blinking suppression is manifested by (1) large on-time fractions and (2) "gray" off states that display appreciable QY. The increase in off-state QY in thick-shelled CdSe/CdS QDs may be a unique feature associated with suppression of Auger[42] or other recombination rates due the band-edge electronic structure in such QDs, and is not observed here. Thick shells can also be effective in spatially isolating the core from the surface, as is reflected in ensemble measurements that show reduced sensitivity of QY to surface ligand-exchange reactions in CdSe/CdS QDs for 19 ML shell thickness,[15] and this has been invoked in explaining the high on-time fractions noted among subpopulations in thick-shell CdSe/CdS QD samples. Here we have found that a high on-time fraction is achievable in QDs with thinner shells, given adequate surface passivation; as seen below, these shells do not isolate the excited state from the surface.

Ligand exchange and aqueous PL QY

Figure 3(a) depicts two strategies that we have explored for bringing the hydrophobically capped QDs described above into aqueous solution via ligand exchange, both as a means towards the use of these QDs in biological imaging applications and as a way to explore the effect of different surface terminations on their photophysical properties – particularly the QY. The first system consists of PEGylated dihydrolipoic acid (DHLA-PEG) small-molecule ligands that are designed to coordinate the QD surface via the thiol groups. The second system consists of polymeric imidazole ligands (PILs): acrylic copolymers that are designed to chelate the QD surface via imidazole sidechains in a manner analogous to poly-histidine peptide domains[43] and PEGylated sidechains that provide water solubility. We have described each of these systems and their preparation previously.[7,6]

Samples **1B** and **1B-ZnS** were ligand exchanged with DHLA-PEG (PEG8, 80% hydroxyl terminated, 20% amine-terminated) and PIL ligands (a random copolymer of 50% methoxy-PEG-11, 50% imidazole sidechains) as described previously,[7,6] yielding well-dispersed aqueous solutions. The absorption and fluorescence lineshapes of the ligand exchanged QDs were essentially unchanged versus those prior to ligand exchange. Dilute solutions of the resulting hydrophilic QDs were prepared in phosphate buffered saline (PBS) for quantum yield measurements.

Figure 3(b) displays the relative quantum yield of these samples, using sample **1B** diluted in octane as the reference (absolute QY >95%). The CdSe/CdS core/shell QDs experienced a dramatic quench of their relative PL QY to just 8% upon ligand exchange with thiol-bearing DHLA-PEG. While even a single thiol ligand can cause a measurable quench of CdSe QD fluorescence,[44] we have previously shown that the DHLA-PEG ligand yields aqueous absolute QYs of 30–40% when used on CdSe/$Cd_{0.2}Zn_{0.8}S$ core/shell QDs of several ML

shell thickness.[6] Indeed, the addition of the ZnS shell to form CdSe/CdS/ZnS QDs is able to rescue the QY of DHLA-PEG coated QDs substantially, even though the addition of the ZnS causes a decrease in the relative QY of the starting hydrophobically-coated QDs to 84% versus the CdSe/CdS reference. A remarkably different result is found when the QDs are cap exchanged with the imidazole-bearing PIL ligand. Aqueous PIL-coated CdSe/CdS QDs maintain a relative QY of 61% versus the parent QDs in octane. In general, we have found the absolute QY of the aqueous PIL-coated CdSe/CdS QDs prepared as described here to fall between 50% and 70%. Addition of the ZnS shell does not confer an added benefit. Importantly, the PIL-coated samples are also quite robust and can be stored under ambient lighting and temperature conditions for an extended period (months) with little change in properties.[7] In addition to the organic surface coatings described above, we have prepared silica-coated single CdSe/CdS QDs via an inverse-micelle method (total hydrodynamic diameter was controlled in the range of 20–70 nm) that display ~40% QY in aqueous solution.[45]

Conclusions

We have shown that CdSe/CdS core/shell QDs can be formed that display ensemble QY close to unity (> 95%) in solution using alternating layer addition. The high QY displayed by our QDs is accompanied by a monoexponential PL lifetime. These QDs display short biexciton lifetimes and high modulation depth blinking, but maintain a high on-time fraction. As such, they could be valuable in efforts to reconcile ensemble and single-particle measurements of excited state decay processes in QDs. Due to the small conduction band offset between CdSe and CdS, the QY of CdSe/CdS core/shell QDs with small shell thickness is significantly influenced by the nature of the surface; consequently much biological imaging work with QD has employed ZnS-terminated surfaces,[46] and published work on optimized commercial QDs with near-unity QY has cited examples that include Zn.[20] We have shown that despite such access of the excited state to the surface, suitable ligand exchange chemistry can limit non-radiative recombination in CdS-capped QDs in aqueous solution. By eliminating the need for ZnS shells and micellular encapsulation, CdSe/CdS QDs are able to incorporate a high density of states in the visible spectrum while maintaining small total diameter; these properties are highly desirable in QDs used as biological probes.

Supplementary Material

Refer to Web version on PubMed Central for supplementary material.

Acknowledgments

This research was supported by the NSF-MRSEC program (DMR-0117795) and made use of its shared user facilities; the Harrison Spectroscopy Laboratory; the MIT-Harvard NIH Center for Cancer Nanotechnology Excellence (1U54-CA119349) (M.G.B.); and the Army Research Office (W911NF-06-1-0101) (D.G.N.). W.L. was supported by a National Science Foundation Graduate Research Fellowship. A.B.G. was a Novartis fellow of the Life Sciences Research Foundation. We thank Ou Chen for helpful discussions.

Notes and references

1. Murray CB, Nirmal M, Norris DJ, Bawendi MG. Zeitschrift Fur Physik D-Atoms Molecules and Clusters. 1993; 26:S231–S233.
2. Smith AM, Nie S. Nat Biotech. 2009; 27:732–733.
3. Kim S, Lim YT, Soltesz EG, De Grand AM, Lee J, Nakayama A, Parker JA, Mihaljevic T, Laurence RG, Dor DM, Cohn LH, Bawendi MG, Frangioni JV. Nat Biotechnol. 2004; 22:93–7. [PubMed: 14661026]
4. Bruchez M, Moronne M, Gin P, Weiss S, Alivisatos AP. Science. 1998; 281:2013–2016. [PubMed: 9748157]
5. Somers RC, Bawendi MG, Nocera DG. Chemical Society Reviews. 2007; 36:579–591. [PubMed: 17387407]
6. Liu W, Howarth M, Greytak AB, Zheng Y, Nocera DG, Ting AY, Bawendi MG. J Am Chem Soc. 2008; 130:1274–1284. [PubMed: 18177042]
7. Liu W, Greytak AB, Lee J, Wong CR, Park J, Marshall LF, Jiang W, Curtin PN, Ting AY, Nocera DG, Fukumura D, Jain RK, Bawendi MG. Journal of the American Chemical Society. 2010; 132:472–483. [PubMed: 20025223]
8. Pons T, Mattoussi H. Ann Biomed Eng. 2009; 37:1934–1959. [PubMed: 19521775]
9. Murcia MJ, Minner DE, Mustata GM, Ritchie K, Naumann CA. J Am Chem Soc. 2008; 130:15054–15062. [PubMed: 18937457]
10. Kim SW, Zimmer JP, Ohnishi S, Tracy JB, Frangioni JV, Bawendi MG. Journal of the American Chemical Society. 2005; 127:10526–10532. [PubMed: 16045339]
11. Hines MA, Guyot-Sionnest P. Journal of Physical Chemistry. 1996; 100:468–471.
12. Peng X, Schlamp MC, Kadavanich AV, Alivisatos AP. Journal of the American Chemical Society. 1997; 119:7019–7029.
13. Dabbousi BO, Rodriguez-Viejo J, Mikulec FV, Heine JR, Mattoussi H, Ober R, Jensen KF, Bawendi MG. The Journal of Physical Chemistry B. 1997; 101:9463–9475.
14. Kortan AR, Hull R, Opila RL, Bawendi MG, Steigerwald ML, Carroll PJ, Brus LE. Journal of the American Chemical Society. 1990; 112:1327–1332.
15. Chen Y, Vela J, Htoon H, Casson JL, Werder DJ, Bussian DA, Klimov VI, Hollingsworth JA. J Am Chem Soc. 2008; 130:5026–5027. [PubMed: 18355011]
16. Talapin DV, Koeppe R, Gotzinger S, Kornowski A, Lupton JM, Rogach AL, Benson O, Feldmann J, Weller H. Nano Letters. 2003; 3:1677–1681.
17. Xie R, Kolb U, Li J, Basche T, Mews A. J Am Chem Soc. 2005; 127:7480–7488. [PubMed: 15898798]
18. Li JJ, Wang YA, Guo WZ, Keay JC, Mishima TD, Johnson MB, Peng XG. J Am Chem Soc. 2003; 125:12567–12575. [PubMed: 14531702]
19. van Embden J, Jasieniak J, Mulvaney P. Journal of the American Chemical Society. 2009; 131:14299–14309. [PubMed: 19754114]
20. McBride J, Treadway J, Feldman LC, Pennycook SJ, Rosenthal SJ. Nano Letters. 2006; 6:1496–1501. [PubMed: 16834437]
21. Mahler B, Spinicelli P, Buil S, Quelin X, Hermier JP, Dubertret B. Nat Mater. 2008; 7:659–664. [PubMed: 18568030]
22. Efros AL, Rosen M. Phys Rev Lett. 1997; 78:1110.
23. Frantsuzov PA, Volkán-Kacsó S, Jankó B. Phys Rev Lett. 2009; 103:207402. [PubMed: 20366010]
24. Spinicelli P, Buil S, Quelin X, Mahler B, Dubertret B, Hermier JP. Physical Review Letters. 2009; 102:136801. [PubMed: 19392384]
25. Mahler B, Lequeux N, Dubertret B. Journal of the American Chemical Society. 2010; 132:953–959. [PubMed: 20043669]
26. Jha PP, Guyot-Sionnest P. ACS Nano. 2009; 3:1011–1015. [PubMed: 19341263]
27. Pandey A, Guyot-Sionnest P. J Chem Phys. 2007; 127:104710–10. [PubMed: 17867772]

28. Nicolau YF. Applied Surface Science. 1985; 22:1061–1074.
29. Park S, Clark BL, Keszler DA, Bender JP, Wager JF, Reynolds TA, Herman GS. Science. 2002; 297:65. [PubMed: 12098690]
30. Allen PM, Walker BJ, Bawendi MG. Angewandte Chemie International Edition. 2010; 49:760–762.
31. Caldwell MA, Albers AE, Levy SC, Pick TE, Cohen BE, Helms BA, Milliron DJ. Chem Commun. 2011; 47:556–558.
32. Kuno, MK. PhD Thesis. MIT; 1998.
33. Leatherdale CA, Woo WK, Mikulec FV, Bawendi MG. Journal of Physical Chemistry B. 2002; 106:7619–7622.
34. Sze, SM. Physics of Semiconductor Devices. John Wiley & Sons; 1981.
35. Schlegel G, Bohnenberger J, Potapova I, Mews A. Phys Rev Lett. 2002; 88:137401. [PubMed: 11955124]
36. Fisher BR, Eisler HJ, Stott NE, Bawendi MG. Journal of Physical Chemistry B. 2004; 108:143–148.
37. Efros AL, Rosen M, Kuno M, Nirmal M, Norris DJ, Bawendi M. Phys Rev B. 1996; 54:4843–4856.
38. Klimov VI, Mikhailovsky AA, Xu S, Malko A, Hollingsworth JA, Leatherdale CA, Eisler HJ, Bawendi MG. Science. 2000; 290:314–317. [PubMed: 11030645]
39. Fisher B, Caruge JM, Zehnder D, Bawendi M. Phys Rev Lett. 2005; 94:087403. [PubMed: 15783930]
40. Knappenberger KL, Wong DB, Romanyuk YE, Leone SR. Nano Lett. 2007; 7:3869–3874. [PubMed: 17994781]
41. Gomez DE, van Embden J, Mulvaney P, Fernée MJ, Rubinsztein-Dunlop H. ACS Nano. 2009; 3:2281–2287. [PubMed: 19655720]
42. García-Santamaría F, Chen Y, Vela J, Schaller RD, Hollingsworth JA, Klimov VI. Nano Letters. 2009; 9:3482–3488. [PubMed: 19505082]
43. Goldman ER, Medintz IL, Hayhurst A, Anderson GP, Mauro JM, Iverson BL, Georgiou G, Mattoussi H. Analytica Chimica Acta. 2005; 534:63–67.
44. Munro AM, Ginger DS. Nano Letters. 2008; 8:2585–2590. [PubMed: 18578549]
45. Popović Z, Liu W, Chauhan VP, Lee J, Wong C, Greytak AB, Insin N, Nocera DG, Fukumura D, Jain RK, Bawendi MG. Angewandte Chemie International Edition. 2010; 49:8649–8652.
46. Medintz IL, Uyeda HT, Goldman ER, Mattoussi H. Nat Mater. 2005; 4:435–46. [PubMed: 15928695]

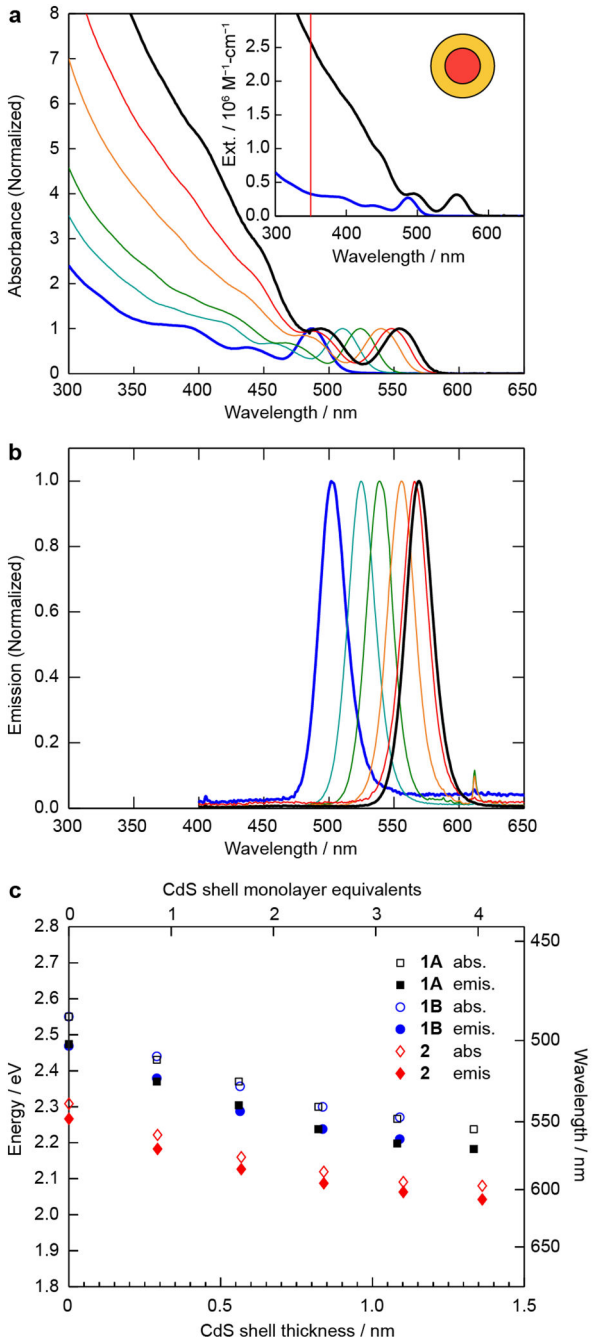

Fig. 1.

Shift in absorption and emission spectral features of CdSe QDs as a result of CdS shell growth. **(a)** Absorption spectra of aliquots withdrawn during preparation of sample **1A** with 0, 0.8, 1.6, 2.4, 3.2, and 4.0 ML equivalents of CdS added. Spectra are scaled such that the height of the lowest-energy exciton peak is equal to 1. Inset: Spectra at start and end of shell growth scaled to reflect the calculated molar extinction coefficient at 350 nm. **(b)** Photoluminescence (PL) spectra of samples in **(a)** excited at 365 nm and scaled to a peak

value of 1. **(c)** Plot of lowest-energy exciton absorption and PL peak positions as a function of targeted CdS shell thickness for the three samples described in Table 1.

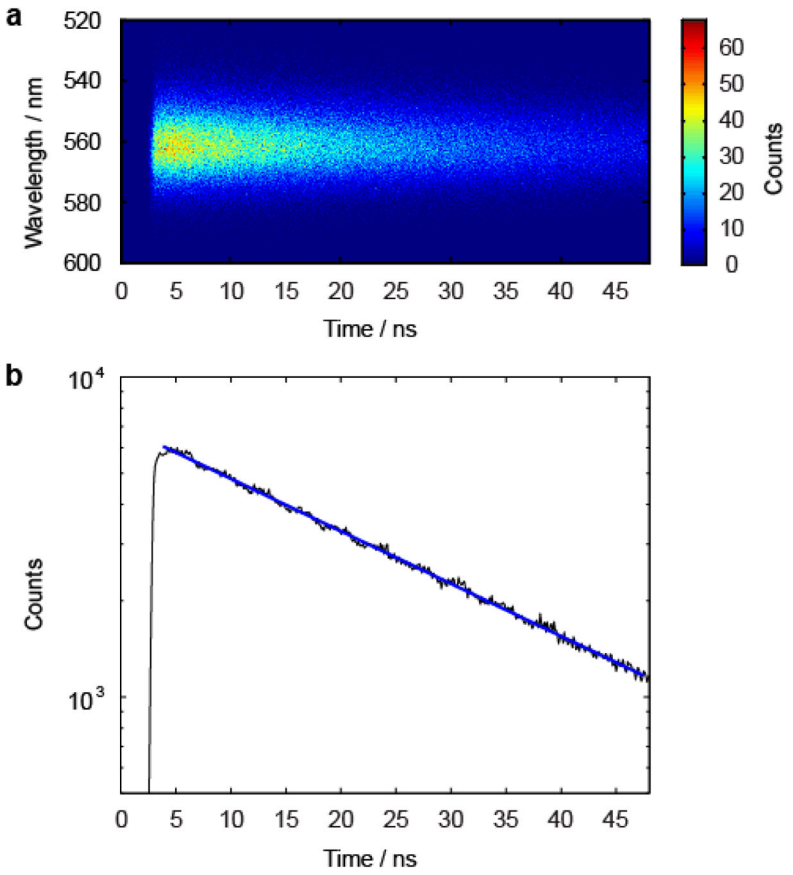

Fig. 2.

(a) Time-resolved PL decay of sample **1B** in hexane solution. (b) Decay trace obtained by integrating from 550 to 570 nm (thin black line). Monoexponential fit with τ_D = 26 ns (thick blue line).

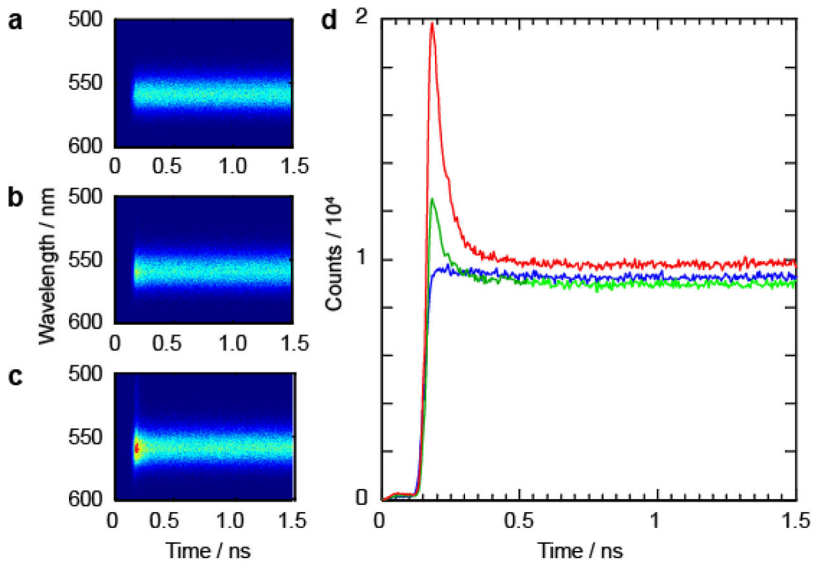

Fig. 3.

PL decay of sample **1B** in hexane excited with 400 nm light. Average pulse energy densities are **(a–c)** 7.7, 55 and 230 μJ/cm^2, corresponding to average excitation densities $n \approx 0.07$, 0.5, and 2 respectively. **(d)** Decay of intensity integrated over a 550–570 nm window for the results shown in **(a–c)**.

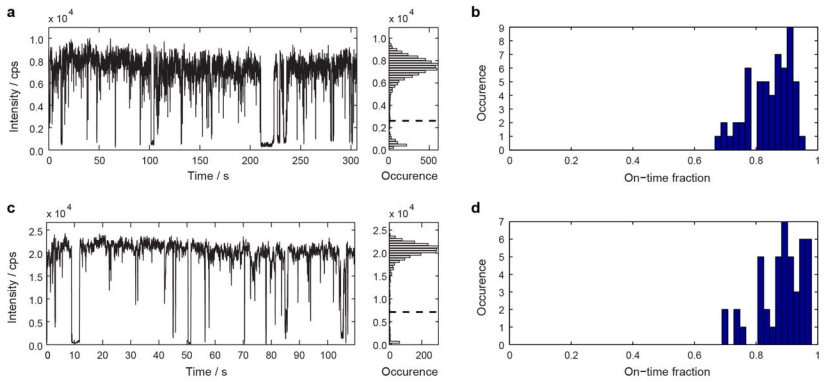

Fig. 4.

Blinking behavior of **1A** (570 nm emission peak, (**a**) and (**b**)) and **2** (610 nm emission peak, (**c**) and (**d**)) under 514 nm CW excitation. **(a,c)** Left: Intensity traces for representative QDs. Right: Distribution of intensities observed over time for these individual QDs. The dashed line indicates the value chosen to demark “on” and “off” states in calculating the on-time fraction. On-time fractions for **(a)** and **(c)** are 90% and 93%, respectively. **(b,d)** Histograms indicating the distribution of on-time fractions among QDs observed in each sample. The total number of QDs observed is 56 and 45 in **(b)** and **(d)**, respectively.

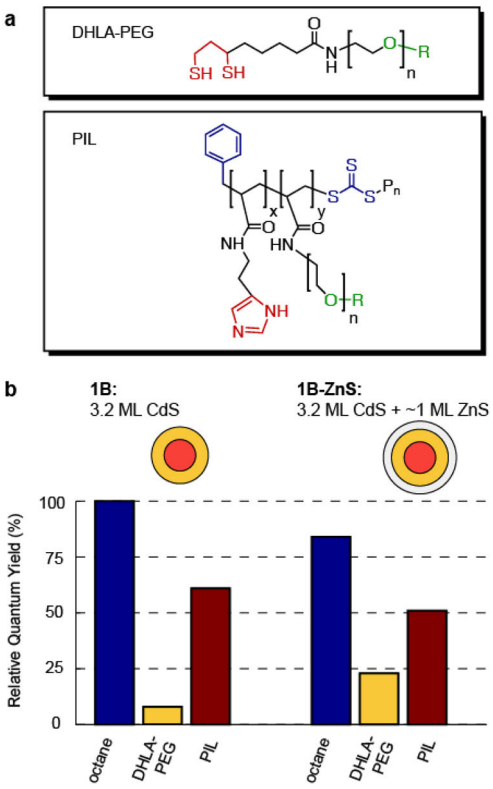

Fig. 5.

(a) General structure of hydrophilic ligands used to prepare aqueous QD samples. **(b)** Effect of ZnS shell growth and ligand exchange on QY of CdSe/CdS core/shell QDs. The relative QY is with sample **1B** diluted in octane as a reference; the absolute QY of this sample was >95%.

Table 1

QD samples discussed in the text.

Sample	CdSe core properties				Overcoated QD properties			
	λ_{abs} (nm)[a]	λ_{em}/fwhm (nm)	Radius (nm, est[b])	ε_{350} ($M^{-1}cm^{-1}$)[c]		λ_{abs} (nm)	λ_{em}/fwhm (nm)	ε_{350} ($M^{-1}cm^{-1}$)
1A	487	503/25	1.32	3.3×10^5	CdS, 5 cycles	555	570/25	2.6×10^6
1B					CdS, 4 cycles	546	562/27	1.8×10^6
1B-ZnS					CdS, 4 cycles, + ZnS	547	562/27	2.2×10^6
2	538	548/24	1.80	8.5×10^5	CdS, 5 cycles	599	610/32	3.8×10^6

[a] Position of longest-wavelength exciton peak.

[b] Calculated from λabs using calibration curve.

[c] Molar extinction coefficient at 350 nm (calculated).